# Onboard Energy Storage Systems for Resilient Operations During Electrified Railway Power Supply Failures

1st James A. Scott (5)
School of Mechanical, Aerospace
& Civil Engineering
The University of Sheffield
Sheffield, United Kingdom
jascott2@sheffield.ac.uk

2<sup>nd</sup> David I. Fletcher (D)
School of Mechanical, Aerospace
& Civil Engineering
The University of Sheffield
Sheffield, United Kingdom
d.i.fletcher@sheffield.ac.uk

3rd Daniel T. Gladwin Deschool of Electrical & Electronic Engineering The University of Sheffield Sheffield, United Kingdom d.gladwin@sheffield.ac.uk

Abstract—Onboard Energy Storage Systems (OESS) have multiple applications in electrified railways. One such application is in discontinuous electrification where an electric train travels across a route that has some electrified and some non electrified sections. Where this is intentional, the OESS can be optimised for the specific design requirement. However, when a normally electrified route experiences a power failure in the Traction Power Supply System (TPSS) this would stop all electric only trains running. A method of using OESS to reduce delays and cancellations associated with TPSS failures is presented and a case study performed using a model developed for discontinuous electrification. A moderately sized 50kWh OESS can be used to allow resilient operation over failed sections approximately 6km in length, when simulated to have 55% of the route in a failed state. A small delay is incurred compared to the normal timetable when using the OESS however this can be compensated through changes to driver behaviour. The results presented here show utilisation of a small energy store greatly enhances resilience of electric railways when failures occur.

Index Terms—Rail, Transport, Electrification, Energy Storage Systems, Power Supply Systems, Resilience

## I. INTRODUCTION

Railways form part of Critical National Infrastructure (CNI) and play a vital role in the economy and lives of people who depend on them. Electric railways by their nature are dependent upon an electric supply in order for them to operate, and failures within this supply system cause disruption to operations and activities. These failures in the Traction Power Supply Systems (TPSS) can be as a result of sabotage as well as more commonly simply mechanical or electrical failures. Previous research and commercial products have shown that Independently-Powered Electric Multiple Units (IPEMUs) [1], [2], which contain their own Onboard Energy Storage Systems (OESS), are capable of powering an electric train through unelectrified sections of railway.

The Authors would like to thank the Engineering and Physical Sciences Research Council (EPSRC) for financial support through their University of Sheffield Doctoral Training Partnership grant EP/T517835/1. The authors also thank Network Rail Infrastructure Limited for their financial and supervisory support to undertake this research.

Across the Great Britain railway network, 2.94x10<sup>5</sup> delay minutes [3] between 2023 and 2024 can be attributable to Overhead Line Equipment (OHLE) or 3rd Rail failures on electrified routes, out of 1.55x10<sup>7</sup> delay minutes from all causes across the whole network. OHLE or 3rd rail faults account for 11% of delay causes from "Non-Track Assets", which itself is attributable for 19.5% of delay minutes across the GB network. However only 39% of the network is electrified [4] [5] and therefore further electrification schemes could see a rise in delays and cancellations due to power failures.

Bi-Mode units that carry an additional diesel generator for routes that are partially electrified may be able to continue their journey should the electrical conductor infrastructure remain intact. However under UK's Traction Decarbonisation Network Strategy (TDNS) [6], reliance on diesel traction is to be reduced and removed entirely. Some routes that contain underground tunnel sections have restrictions on zero emission traction when underground. OESS such as battery storage offers a solution to an alternative redundancy level that do not have emissions and can be utilized on electrified railways to facilitate resilient operations.

# II. METHODOLOGY

# A. Traction Power Supply Systems

An overview of the TPSS is shown in Figure 1 highlighting the flow of energy between the onboard systems for the traction motors as well as the associated lineside infrastructure. The role of the Onboard Energy Storage Systems (OESS) can be shown to be able to charge from both the conductor rail or OHLE and also from regenerated energy from the traction motors. Lineside Energy Storage Systems (LESS) are included in the system overview however these are not necessarily incorporated in the real life solution or in the model.

This ability to charge the OESS from either the electrical power supply or from the motors during regenerative braking is shown again in Figure 2. Class 777/1s [1], [2] are in passenger revenue service with Merseyrail operating on a DC network with an OESS for unelectrified expansions to the

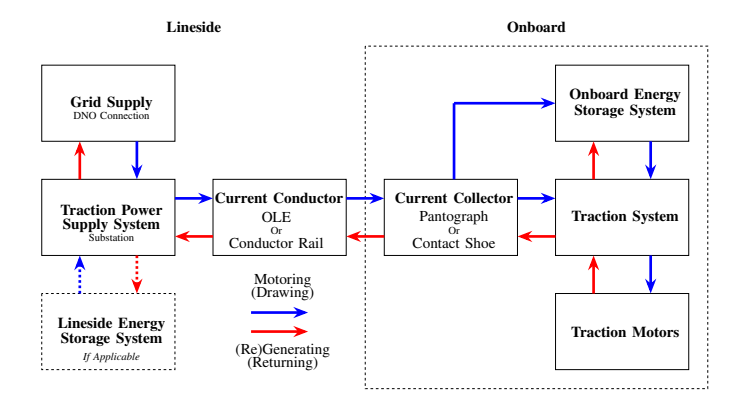


Fig. 1: System Overview of Traction Power Supply Systems (TPSS) and Energy Flows, both for Onboard Energy Storage Systems and Lineside Energy Storage Systems (LESS).

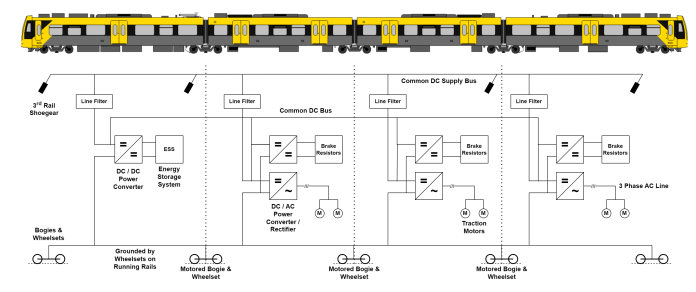


Fig. 2: Electrical Architecture for the Traction Power Systems of a Merseyrail Class 777/1 with Onboard Energy Storage Systems

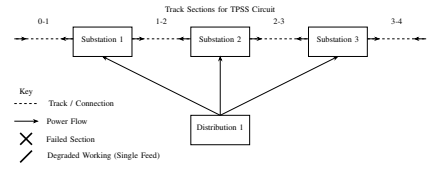
network. There is a common DC bus that links the Energy Storage System (ESS) with the rectifiers and inverters for the traction motors. Brake resistors are also used for conventional regenerative braking with no energy recovery.

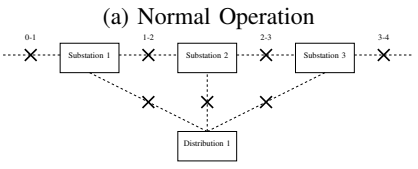
### B. Substation Failure Mechanisms

A number of failure mechanisms have been identified, as shown in Figure 3 as possible ways the electrical supply may be disrupted. The normal case is represented in Figure 3a showing how the substations are normally configured with track sections receiving a double feed from both ends from individual substations. These substations are connected to a distribution network powered from the National Grid [7]. Failures where the distribution network has failed as shown in Figures 3b, 3c & 3d or local substation failures as in Figures 3e, 3f, 3g & 3h. Some failure cases offer a potential for degraded working conditions where the power is delivered either by a single feed, where it would otherwise be double fed, as in Figures 3c, 3f or 3g, or a double feed over an extended length of track as in Figures 3d or 3h.

## C. Modelling

A time stepped model previously developed for understanding OESS assisted discontinuous electrification [8] has been expanded to include further substation analysis. Individual

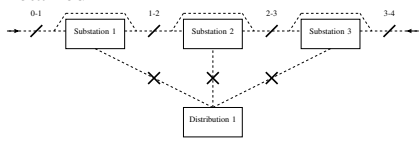




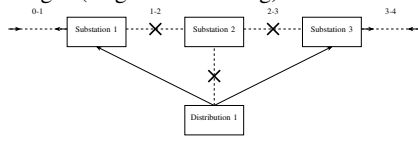
(b) Distribution Failure - Wide Area with Single Feed Capability on 0-1 and 3-4 Unavailable



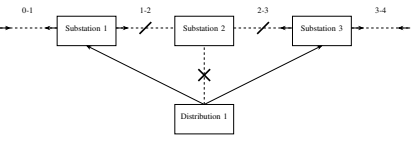
(c) Distribution Failure - Local Area with Single Feed Capability on 0-1 and 3-4 Retained



(d) Distribution Failure with Bridged Sections allowing Double Feed over Extended Length (Degraded Working)



(e) Single Substation Failure - Single Feed Capability Between Substations Unavailable



(f) Single Substation Failure - Single Feed Capability Between Substations Retained



(g) Single Substation Single Side Failure

1.2 2.3 3.4 3.4 Substation 3 3.4 Substation 3 3.4 Substation 1

(h) Single Substation Failure with Bridged Section allowing Double Feed over Extended Length (Degraded Working)

Fig. 3: Substation and Distribution Power Delivery Setups and Failure Cases

substations have been positioned along a sample route representative of a typical DC Third Rail urban / suburban network. Where one substation supplies electricity in both the Up and Down directions as the train travels along the route, this is modelled as two individual substations. These can then be recombined during analysis or failure modes as if acting on that one substation powering both directions [9].

The model is split into three coupled but distinct areas; mechanical, electrical and energy storage systems. Mechanical modelling is derived from kinematic equations which are equated to the electrical model through powers and transmission efficiencies.

Principle time stepped mechanical calculations follow Newtonian kinematic equations as shown in Equation 1 where  $F_{Net}$  is resultant force,  $F_T(v)$  is the traction force as a function of velocity (v), B(v) is the braking force, Q(v) is rolling resistance and  $F_{Grad}$  the force introduced by the track gradient.  $M_{Train}$  is the mass of the train.

$$F_{Net}(v) = F_T(v) + B(v) + Q(v) + F_{Grad}$$

$$= M_{Train} \cdot \frac{dv(t)}{dt}$$
(1)

These forces are then relayed to appropriate powers (P) and energies (E) for either Traction  $(P_T, E_T)$  or Regeneration  $(P_R, E_R)$  in Equations 2 & 3 where  $\eta_{PT}$  &  $\eta_R$  are the efficiencies of the power train and regeneration respectively [10]–[15].

$$E_T = \int P_T dt = \int \frac{F_T(v) \cdot v}{\eta_{PT}} dt$$
 (2)

$$E_R = \int P_R dt = \int -B(v) \cdot v \cdot \eta_R dt \tag{3}$$

These powers and energies only account for the mechanical, or kinematic, traction and regeneration of the train and do not consider the additional power consumption of any hotel loads  $(P_H)$  or the impact of charging the OESS  $(E_{Add})$  by drawing additional power from the conductor rail or returning less to the rail from the regenerated energy. Equations 4 & 5 implement these additional draws and reductions in returns to show the power transmission at the point of contact between the current collector and the conductor rail (3rd rail) or conductor cable (OHLE), where  $P_{Req2D}$  is the required power to draw and  $P_{Reg2R}$  is the regenerated power to return.

$$P_{Req2D} = P_T + P_H + \frac{d}{dt} E_{Add} \tag{4}$$

$$P_{Reg2R} = P_R - P_H - \frac{d}{dt} E_{Add} \tag{5}$$

Substations are modelled as Thevenin equivalent circuits [12], [16], [17], with one voltage source  $(V_{s1} \& V_{s2})$  and an equivalent, internal resistance  $(R_{s1} \& R_{s2})$ . Figure 4 shows the equivalent circuit with variable resistors to account for the change in the resistance of the conductor rail as the train progresses along the line  $(R_{T1} \& R_{T2})$ . Key specifications for

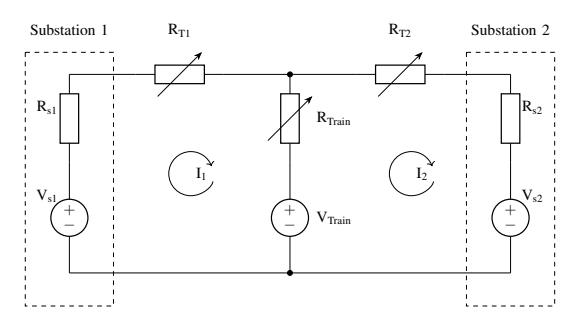


Fig. 4: An Equivalent Circuit for a Train either Drawing or Returning Electrical Power from a Conductor Rail Between Two Substations in a Double Feed Configuration

| Parameter                  | Symbol           | Value   | Unit              |
|----------------------------|------------------|---------|-------------------|
| Line Voltage               | $V_{s1}, V_{s2}$ | 750     | V                 |
| Substation Resistance      | $R_{s1},R_{s2}$  | 0.2     | Ω                 |
| Regeneration Voltage       | $V_R$            | 800     | V                 |
| Conductor Rail Resistivity | $ ho_{ m Track}$ | 0.04061 | Ωkm <sup>-1</sup> |
| Hotel Power                | $P_{\mathrm{H}}$ | 50      | kW                |
| OESS Energy Density        | $\rho_{ m OESS}$ | 100     | Whkg-1            |
| OESS Charge Rate           | $C_{Charge}$     | 5       | -                 |
| OESS Discharge Rate        | $C_{Discharge}$  | 10      | -                 |

TABLE I: Key Electrical Specifications

the values of the voltage sources, substation resistances, hotel power and resistivity of the conductor rail [12] are shown in Table I. The train is represented by a variable resistance, where  $R_{Train(D)}$  &  $R_{Train(R)}$  are train resistances for drawing and regeneration respectively, dictated by the power being either returned or drawn from the rail in Equations 9 & 10, where  $V_{Train}$  is the voltage at the train if regenerating or 0V if drawing power and  $V_{Line}$  is the line voltage at the shoe as seen by the train. Corresponding currents ( $I_1$  &  $I_2$ ) are calculated from Kirchoff loop analysis using Equations 6, 7 & 8.

$$\mathbf{V} = \begin{bmatrix} V_{s1} - V_{\text{Train}} \\ V_{\text{Train}} - V_{s2} \end{bmatrix} \tag{6}$$

$$\mathbf{R} = \begin{bmatrix} R_{\text{s}1} + R_{\text{T1}} + R_{\text{Train}} & R_{\text{Train}} \\ -R_{\text{Train}} & R_{\text{s}2} + R_{\text{T2}} + R_{\text{Train}} \end{bmatrix}$$
(7)

$$\mathbf{I} = \begin{bmatrix} I_1 \\ I_2 \end{bmatrix} = \mathbf{R}^{-1} \mathbf{V} \tag{8}$$

$$R_{Train(D)} = \frac{V_{Line}^2}{P_{Req2D}} \tag{9}$$

$$R_{Train(R)} = \frac{V_R(V_R - V_{Line})}{P_{Reg2R}}$$
 (10)

Where a train is in a single feed, or single stub, section, the model represents this by changing the voltage source to 0V and changing the internal impedance to  $1M\Omega$  to have no power delivery but to also avoid a short circuit. To implement substation failures as in Figure 3, the model simply manipulates the ability of the train to see the electrical infrastructure from its reference. Control boundaries for the electrical infrastructure

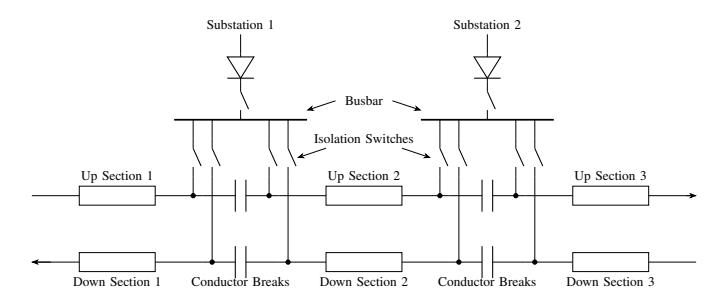


Fig. 5: Typical DC Substation Feeder Arrangement for Bi-Directional Track

and OESS are indicated in Figure 6 which also shows the losses associated with the OESS and electrical infrastructure. The energy store is modelled as a "Bucket Model" [18] [19] which allows a configurable energy storage system that can be characterised to multiple different energy storage systems such as batteries, supercapacitors or hybrid systems. This has the advantage of allowing interchangeability and is readily reconfigurable without the need for complex equivalent circuits. Efficiencies are applied to both charging and discharging as shown in Figure 6. The charging and discharging algorithm based on the OESS State of Charge (SoC) to dictate how much is added or removed is shown in Equations 11 & 12, where  $E_{Add}$  &  $E_{Rem}$  is the energy being added or subtracted from the OESS.

$$E_{Max \ Add} = SoC < 0.7 \&$$

$$E_{CR} = E_{CR} = E_{CR}$$

$$E_{Max\ Add} = OESS\ Capacity\ (Wh) \cdot C_{Charge} \cdot dt$$
 (13)

(14)

 $E_{Max\ Rem} = OESS\ Capacity\ (Wh) \cdot C_{Discharge} \cdot dt$ 

| Physical<br>Substation<br>No. | Model<br>Substation<br>Up No. | Model<br>Substation<br>Down No. | Fail<br>Case | Track<br>Affected<br>(km) |
|-------------------------------|-------------------------------|---------------------------------|--------------|---------------------------|
| 1                             | 1                             | 14                              | No           | -                         |
| 2                             | 2                             | 13                              | Yes          | 5.26                      |
| 3                             | 3                             | 12                              | No           | -                         |
| 4                             | 4                             | 11                              | No           | -                         |
| 5                             | 5                             | 10                              | Yes          | 4.45                      |
| 6                             | 6                             | 9                               | No           | -                         |
| 7                             | 7                             | 8                               | No           | _                         |

TABLE II: Paired and Failed Substations

Where  $\eta$  represents the losses in and out of the OESS,  $E_R$  is  $P_R \cdot dt$ ,  $E_H P_H \cdot dt$ , the energy required  $E_{Req} = (P_T + P_H) \cdot dt$ ,  $E_{Max\ Add}$  is the maximum energy to be added to the OESS as detailed in Equation 13 and  $E_{Max\ Rem}$  is the maximum energy to be removed from the OESS as detailed in Equation 14.

The energy flows in Figure 6 extrapolate on the TPSS overview in Figure 1, but without LESS, and are representative of the electrical architecture in Figure 2.

### III. CASE STUDY

As this study is investigating the impact of damaged or non-working Critical National Infrastructure (CNI), the case study has been based on a real line however the location of CNI instalments such as substations have been altered such that no sensitive material is available from this paper. As such the location of substations in this investigation are based on an approximate system, and the case study route is typical of that of a 3rd rail DC urban / suburban commuter line.

The case study route is a standard bi-directional line where substations power both of the conductor rails in both directions and with substation feeding arrangements as shown in Figure 5 [20]. The case study line also includes a single track, unidirectional section to represent an underground tunnel core section. In this case the substation supplies only one track.

On the case study route the individual bi-track substations are represented as two uni-track substations each feeding in both directions. For failures on bi-track configurations they are paired with the appropriate corresponding substation for the reverse direction. The case route uses 16 substations along a route approximately 35km long. Each substation is separated by approximately 2km - 6km of track.

The failures represented in this study are as shown in Figure 3e where a single substation failure inhibits the draw of electricity from the neighbouring substations and degraded working over from either a single feed or extended double feed with bridged sections is unavailable. This represents a worst case scenario for a single substation failure. The paired substations and those which have are simulated to have failed are shown in Table II.

The case study uses rolling stock similar in characteristics to a Merseyrail Class 777, with an OESS having a high power capability but low overall capacity. This is characterized as a 50kWh store with a charge rate of 5C and discharge rate of 10C. The Class 777 is a Electric Multiple Unit (EMU) in passenger operating service within the UK on urban and

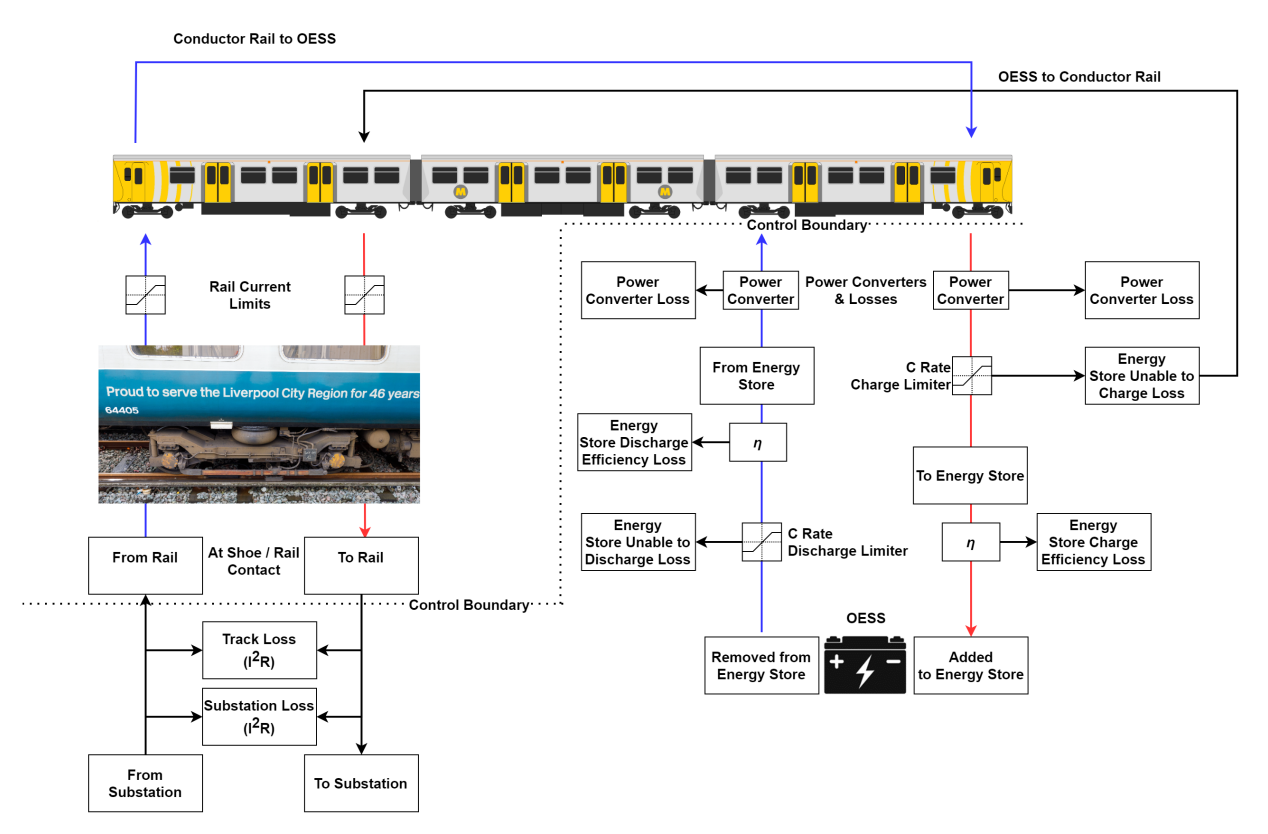


Fig. 6: Modelled Energy Flows and Losses from the TPSS, OESS and Substations

suburban lines making it a good candidate to base a model off. The Class 777/1 variant has a 320kWh LTO-NMC battery onboard however for this resilience investigation a smaller store, as detailed earlier, is used to reduce the weight and show the concept of a resilient system.

# IV. RESULTS & FURTHER WORK

The model was run with the failed substations as detailed in Table II, with model parameters for the OESS and electrical systems as listed in Table I and the resulting output of the OESS State of Charge (SoC) for an OESS of 50kWh and individual substation current as in Figure 7. The middle plot shows the SoC which has a basic management system controlling its charging and discharging. Individual currents from substations can be seen in the bottom plot with the sections of unpowered track with a notable absence in their substation currents.

The model took approximately 180 seconds to run on a laptop with an Intel i9 processor with 32 GB of RAM for a single train simulation. The failures of the substations are as in Figure 3e where an individual substation has failed with no degraded working conditions such as bridging or single feeds from neighbouring substations. This was the only fail case to be investigated in this study and further failure types will be investigated in due course.

The model was initially calibrated to complete the fully electrified journey in 3960 seconds, as based on the Working Timetable (WTT) of the case study route. For the scenario

involving the failures the driver behaviour was kept identical to that of the normal case, in comparison, when the substations were failed the route was completed in 4286 seconds. This represents a journey that is approximately 6 minutes longer than the timetabled service as running from the OESS doesn't deliver as much power as the conductor rail to be able to keep to the WTT. However, using the OESS prevents a cancellation due to a TPSS failure that would have stopped services operating without an OESS in a resilience capacity.

The length of track affected by each failure is detailed in Table II, for a complete route this gives 19.42km of unelectrified track out of a case study route of 35km. This means the service is required to run on the OESS for 55.6% of the route. Normally if over half of the route was unelectrified this would be impossible for any electric only trains to operate.

The SoC and velocity profile as show in in Figure 7 illustrates that when running on this 50kWh store, which is power dense but doesn't have as high of a capacity as a 320kWh store for prolonged running on the OESS, the velocity profile alters to having poorer acceleration and reductions in the maximum line speed achieved. This contributes to the longer travel time when operating using the OESS over sections of track without electrical power.

Differing combinations of specific power and energy density for the OESS will yield differing results. For instance if this test route were to be run again with a 320kWh store, but with the same C rates, the delay from running off the OESS would

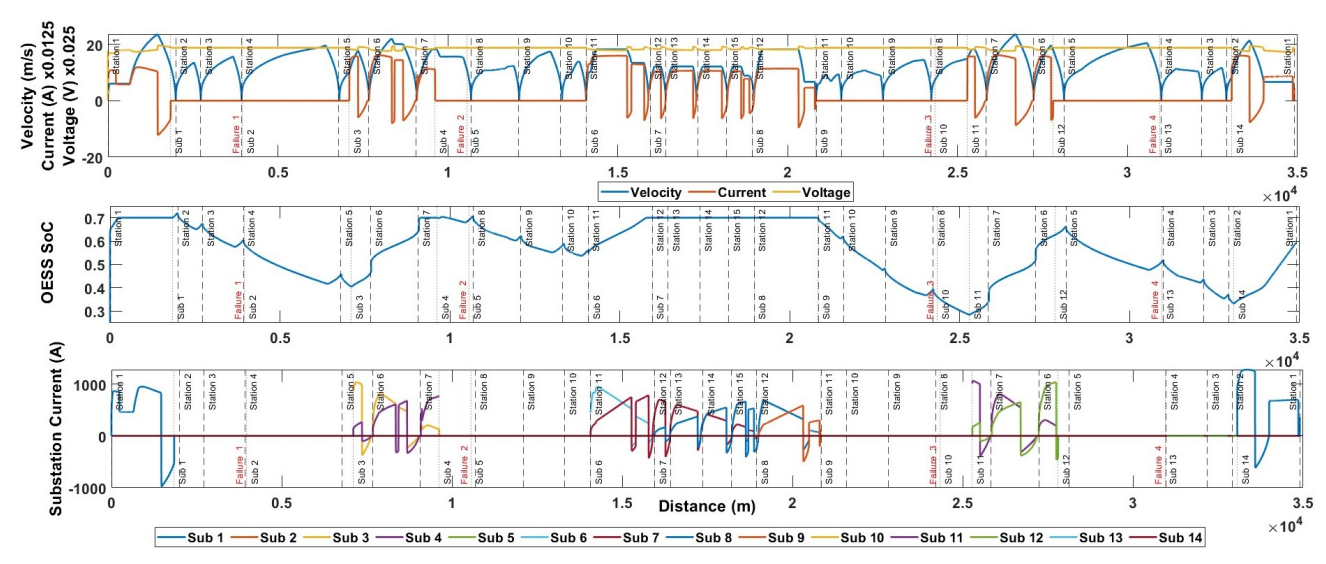


Fig. 7: OESS State of Charge with Current from Each Substation Alongside the Kinematic Trajectory of the Train Along the Case Study Line with 2 Failed Substations, Impacting 4 Electrical Sections of Track

be less than with the 50kWh store. This is due to the rate of power delivery being proportional to the size of the store, a larger store can deliver more power for the same C rate.

Larger onboard stores will be able to cope with longer lengths of unelectrified track but at the expense of carrying an additional mass onboard that could be infrequently used. Smaller stores to cope with small outages cannot replicate the performance of the fully electrified system and incur delays, however this trade off could be beneficial to avoid cancellations of journeys and maintain an operational system.

OESSs add an additional weight cost and increase both the initial and operational costs of the train. A trade-off exists between the cost of the upkeep and maintenance of lineside infrastructure to make the power systems more reliable or operating in failure cases, the cost of installing and operating OESS on EMUs and the cost of the impact of a power outage affecting services. As TPSS can be considered CNI, the impact or cost of a power failure in a critical TPSS system could be greater than the OESS cost. This is an area for future investigation to determine the optimum size and specification of the OESS along with consideration for the capital and operation expenditure it will require.

## ACKNOWLEDGMENT

The authors are grateful for support from Stephen Phillips at Siemens Rail Infrastructure, Siemens Motability, Sheen Matthews at Merseyrail Electrics, Merseyrail Electrics, Great Western Railway and Richard Stainton at Network Rail Infrastructure Limited.

# REFERENCES

- [1] Stadler, "Metro Merseyrail EMU Class 777/0," 2022.
- [2] Stadler, "Metro Merseyrail IPEMU Class 777/1," 2022.
- [3] ORR, "Passenger Rail Performance Statistical Release," 2025.
- [4] ORR, "Rail Environment," 25-01-2025 2024.
- [5] ORR, "Rail Infrastructure and Assets," 25-01-2025 2024.

- [6] Network Rail, "Traction Decarbonisation Network Strategy," report, 2020.
- [7] F. Kiessling, Contact lines for electrical railways: planning, design, implementation, maintenance. Erlangen: Erlangen: Publicis Pub., 2009, 2nd revision ed., 2009.
- [8] J. Scott, D. Fletcher, and D. Gladwin, "Onboard Energy Storage for Discontinuous, Safer Third Rail DC Electrified Rail Systems," Proceedings of the Institution of Mechanical Engineers, Part F: Journal of Rail and Rapid Transit. 2025.
- [9] M. Brenna, F. Foiadelli, and D. Zaninelli, Electrical Railway Transportation Systems. Piscatawaya, New Jersey: Piscatawaya, New Jersey: Wiley-IEEE Press, 2018, 2018.
- [10] M. Spiryagin, S. Bruni, C. Bosomworth, P. Wolfs, and C. Cole, *Rail Vehicle Mechatronics*. Boca Raton: Boca Raton: CRC Press, 2022, 2022.
- [11] A. Sładkowski, Railway Transport Systems Approach. Cham, Switzerland: Cham, Switzerland: Springer, 2018, 2018.
- [12] D. I. Fletcher, R. F. Harrison, and S. Nallaperuma, "TransEnergy a tool for energy storage optimization, peak power and energy consumption reduction in DC electric railway systems," *Journal of Energy Storage*, vol. 30, p. 101425, 2020.
- [13] H. Alnuman, D. T. Gladwin, and M. P. Foster, "Novel Control Method for Improving Energy Efficiency of DC Electric Railways," in 2019 IEEE 15th International Conference on Control and Automation (ICCA), pp. 91–96.
- [14] H. Alnuman, D. Gladwin, M. Foster, E. M. Ahmed, M. Aly, and A. Alshahir, "Electrical modelling of a metro system," *Electric Power Systems Research*, vol. 213, p. 108680, 2022.
- [15] G. J. Hull, C. Roberts, and S. Hillmansen, "Simulation of energy efficiency improvements on commuter railways," in *IET Conference on Railway Traction Systems (RTS 2010)*, pp. 1–9.
- [16] P. Horowitz and W. Hill, The Art of Electronics. New York, NY, USA: New York, NY, USA: Cambridge University Press, 2015, third edition. ed., 2015.
- [17] B. Tomlinson, "Modelling part of the southern region D.C. distribution network: some electrical data," report, 1987.
- [18] A. J. Hutchinson and D. T. Gladwin, "Verification and analysis of a Battery Energy Storage System model," *Energy Reports*, vol. 8, pp. 41– 47, 2022
- [19] S. J. Royston, D. T. Gladwin, D. A. Stone, R. Ollerenshaw, and P. Clark, "Development and Validation of a Battery Model for Battery Electric Multiple Unit Trains," in *IECON 2019 - 45th Annual Conference of the IEEE Industrial Electronics Society*, vol. 1, pp. 4563–4568.
- [20] E. Stewart, P. Weston, C. Roberts, and S. Hillmansen, "Monitoring the energy consumption in DC railways," in *IET Conference on Railway Traction Systems (RTS 2010)*, pp. 1–4.